



1 Seasonal Sinking rates of Transparent Exopolymer Particles (TEP) concentrations with 2 associated Carbon flux in adjacent Bohai Sea and Yellow Sea

3 M Shahanul Islam^{1,2,3}, Sun Jun^{2,3*}, Li Xiaoqian^{2,3}, Leng Xiaoyun^{2,3}

- 4 1. College of Food Engineering and Biotechnology, Tianjin University of Science and
 5 Technology University, Tianjin 300457, China
- 6 2. Tianjin Key Laboratory of Marine Resources and Chemistry, Tianjin University of
 7 Science and Technology, Tianjin 300457, PR China
- 8 3. Research Centre for Indian Ocean Ecosystem, Tianjin University of Science and
 9 Technology, Tianjin 300457, China

10 *Corresponding Author: phytoplankton@163.com

11 Abstract

12 To study the seasonal transparent exopolymer particles (TEP) distributions,
 13 sedimentation and its impacts on carbon cycle in north Chinese seas, a total of total 56
 14 stations TEP samples and its sinking rate measurements by SETCOL method via water
 15 sampling cruise during autumn (2014), summer (2015) and winter (2015) in the Bohai Sea
 16 (BS), North Yellow Sea (NYS) and South Yellow Sea (SYS) at three different depths were
 17 carried out. Temperature, phytoplankton, chlorophyll-a (Chl-a) and salinity with five
 18 nutrients, phosphate (DIP), silicate (DSi), dissolved inorganic nitrate (DIN) (including nitrite,
 19 nitrate and ammonium) were also collected and measured for correlation analysis to visualize
 20 the seasonal effects on TEP concentrations (CTEP) and its sinking. Average of total CTEP
 21 ($2.13 \mu\text{g Xeq L}^{-1}$) was higher in NYS ($3.32 \mu\text{g Xeq L}^{-1}$) coastal currents with highest average
 22 CTEP during winter ($6.17 \mu\text{g Xeq L}^{-1}$) specially in NYS ($7.00 \mu\text{g Xeq L}^{-1}$) through coastal
 23 current mixing zone. Average of total sinking rates (1.03 mD^{-1}) was higher in SYS (1.09
 24 mD^{-1}) through mid-water layer than other seas, especially in autumn (1.13 mD^{-1}) with higher
 25 seasonal average sinking rates at summer (1.04 mD^{-1}). Carbon associated with TEP (TEP-C)
 26 was averagely distributed ($1.47 \mu\text{g C L}^{-1}$) at subsurface layer of study areas. Seasonal highest
 27 distribution of TEP-C was $4.44 \mu\text{g C L}^{-1}$ during winter, mostly in NYS. Dominant
 28 phytoplankton species *Paralia sulcata*, *Thalassiosira excentrica* and *Rhizosolenia styliformis*
 29 maintained average correspondences with CTEP which may indicate the influences of them
 30 on TEP concentration. Congregating oceanic stations in other groups, coastal stations were
 31 averagely clustered together in multivariate analysis. Average canonical correspondence



analysis showed close relation of CTEP with Chl-a during autumn and with nutrient during winter.

Keywords: Transparent Exopolymer Particles, sinking rate, carbon sink, seasonal variation, Bohai Sea, Yellow Sea.

1 Introduction

Transparent exopolymer particles (TEP) are macro-gels like substances that play an active role in the marine carbon cycle between particulate and dissolved organic carbon (POC and DOC, accordingly), by extending the size continuum, in addition to assisting particle formation (Alldredge et al., 1993; Passow, 2002b; Verdugo et al., 2004). TEP are generally consider as transparent particles which can be stainable by Alcian Blue, a dye that favorably binds to acidic polysaccharides after complexing with carboxyl groups and sulfate (Alldredge et al., 1993; Passow and Alldredge, 1995). Abiotically TEP sourced from dissolved polysaccharides secreted by phytoplankton (Logan et al., 1995; Passow, 2002b; Thuy et al., 2015). As TEP possess surface-active characteristics with neutral buoyancy, they are scavenged easily with gas bubbles and aggregated at the sea surfacelayer which can make sea surface microlayer (SML) organically (Azetsu-Scott and Passow, 2004; Cunliffe et al., 2013; Mopper et al., 1995; Wurl et al., 2009).

A combined effect of regional biological and physical factors, including salinity, air-driven turbulence and production of dissolved polysaccharide primer by phytoplankton and bacteria can controlled the formation and distribution of TEP. Nutrient ranges control phytoplankton community, which is one of the relative factors that thrust the partitioning of organic matter between particulate and dissolved phases (Carlson et al., 1998; Conan et al., 2007; Lomas and Bates, 2004; Thornton, 2014), and organic matter and production of TEP (Claquin et al., 2008; Corzo et al., 2000; Mari et al., 2005; Passow, 2002a). Relationships between TEP and chlorophyll *a* (Chl-a) develop during a bloom, resembles the production of TEP by phytoplankton (Passow, 2002b). This relationship during bloom phase is species-specific, with the cellular aggregation rate of TEP by phytoplankton caused by their growth period. So, if the area is composited with other phytoplankton taxa with different life stages, the relation will not match with special gradient between TEP–Chl-a. Low nutrient increases TEP abundances through preventing TEP consumption by bacteria (Bar-Zeev and Rahav, 2015), so that aggregation and accumulation of TEP at sea surface as N-poor C-rich organic material (Passow, 2002b).



64 In the sea surface microlayer (SML), gel particles formations and abundance have
65 been observed (Orellana et al., 2011; Wurl et al., 2011b) which resembles the relation of gels
66 with carbon cycling at the surface layer. Surface active TEP is transported to the SML after
67 accumulation with rising bubbles derived from wave's action (Wurl et al., 2011a; Wurl and
68 Holmes, 2008). Although these actions distribute its substances into subsurface layer
69 temporarily though SML has a rapid reformation intensity (Cunliffe et al., 2013). Biogenic
70 material concentrated in the SML may also be mixed with atmosphere through bubble
71 rupturing which may capable of ice nucleation and cloud condensation (Bigg and Leck, 2008;
72 DeMott et al., 2015; Orellana et al., 2011; Quinn et al., 2014; Wang et al., 2015; Wilson et
73 al., 2015). Since TEP sticks to elevated bubbles (Mopper et al., 1995) and are accumulated in
74 the SML, TEP may contribute to the organic increment of sea spray aerosols produced from
75 film droplets (Aller et al., 2005).

76 TEP are more adherer than non-TEP substances which may help in particles and
77 subsequently increase sedimentation (Logan et al., 1995; Passow et al., 1994). As microbial
78 hotspots, TEP and POC serve a source of carbon to the deep ocean by sinking in water
79 column. Although sinking process of marine aggregates have been observed (Burd and
80 Jackson, 2009; Iversen and Robert, 2015; Jokulsdottir and Archer, 2016; Prairie et al., 2015),
81 there remains the necessity of understanding about the effect of TEP in the biological carbon
82 pump (Burd et al., 2016; Zetsche and Ploug, 2015). TEP sinking rate measurement
83 experiments in Changjinag (Yangtze River) estuary near EastChina Sea during summer
84 showed higher sedimentation of TEP at upper water layer than deep seas (Guo & Sun 2018).
85 It also showed higher sinking rates of TEP in summer rathe then spring which may have
86 important role about carbon exports in that area.

87 Present study was conducted through the semi-closed Bohai Sea (BS) and Yellow
88 Seawhich covered a big part of the north Chinese seas. Semi enclosed BS is located at the
89 north-eastern continental region of China (Xu et al. 2010). With sensitive primary
90 productivity and commercial fishery (Tang et al. 2003, Huang et al. 1999), BS got waste
91 water-loads and inputs from the Tianjin City as well as Liaoning, Shandong and Hebei
92 provinces (Xu et al. 2010). At eastern of BS, there is another semi-enclosed marginal sea of
93 the western Pacific Ocean which is the Yellow Sea (Liu et al. 2015b). Yellow Sea possesses
94 various oceanic processes through seasons (Hwang et al. 2014; Su 1998; Yuan et al. 2008;
95 Isobe 2008). Visualizing better seasonal scenario, oceanic area of Yellow Sea was divided
96 into two major water body (Li et al. 2017) i.e. North Yellow Sea (NYS) and South Yellow



97 Sea (SYS). In autumn, appearance of Yellow Sea cold water mass (YSCW) at SYS
98 influenced the vertical mixing of NYS water (Zou et al. 1999). The Yellow Sea Warm
99 Current (YSWC) acted at SYS during winter (Gao et al., 2004, Su 1998) and Changjiang
100 Diluted water (CDW) during summer (Naimie et al. 2001). Fishery (Tang and Su, 2001),
101 biological community (Hyun and Kim, 2003; Fu et al., 2009; Zhang et al., 2009) and
102 ecological problems raises the importance of researches on Yellow Sea (Sun et al., 2011;
103 Tang et al., 2007, 2010).

104 Studies on the TEP and its sinking rates showed correlation with environmental
105 parameters i.e. temperature (Claquin et al. 2008, Fukao et al. 2012), salinity (Mari et al. 2012)
106 and phytoplankton species composition (Passow 2002b). On the other hand, it also showed
107 correlation with nutrients in different studies (Corzo et al. 2000, Mari et al. 2005). Seasonal
108 variation of parameters can be a cause behind these phenomena. Poor correlations among
109 TEP and these environmental parameters can be found due to limited data and insignificant
110 variations in salinity and nutrients from sampling stations (Guo & Sun 2018). Seasonal
111 distribution and sinking rate of TEP will describe more specific relation of TEP with other
112 environmental parameters. On the basis of these objectives, present study was conducted on
113 sinking flux of TEP and its concentration with related carbon exports through three separate
114 seasons (autumn, summer, winter) in the Bohai and Yellow Sea of China from 2014-2015.

115 **2 Materials and Methods**

116 **2.1 Study area**

117 Water sample (1 liter) was taken from three different depths (0-100 meters) at various
118 stations (Fig. 1) during 2014-2015 in Bohai Sea (BS), North Yellow Sea (NYS) and South
119 Yellow Sea (SYS). Autumn sampling was conducted between 8-22 November (Fig. 1A),
120 2014, summer sampling from 18 August to 22 September, 2015 (Fig. 1B) and winter
121 sampling in Bohai Sea and North Yellow Sea from 17 October to 22 November, 2015 (Fig.
122 1C). Boundary currents flow directions in Bohai Sea and Yellow Sea were changed with
123 seasons (Fig. 2). Korean coastal currents (KCC) flows northward in summer and southward
124 in winter. YSWC was found during winter and CDW flows eastward during summer. Remain
125 coastal currents and warm currents flows in their constant direction (Hwang et al. 2014; Su
126 1998; Yuan et al. 2008; Isobe 2008) which may have tributary effect on these particles
127 concentration and its sinking rates besides all hydrological parameters.



128 Sampling stations (St.s) of autumn through the Bohai Sea (St.s B45, B49, B57, B62,
129 B68), North Yellow Sea (St.s B04, B11, B15, B19, B25, B34) and South Yellow Sea (St.s
130 H07, H09, H10, H18, H20, H26, H27, H33, H35, H40) were determined by geographical
131 positions. Similarly, the stations of Bohai Sea (St.s B45, B49, B57, B62, B67, B68), North
132 Yellow Sea (St.s B04, B10, B15, B19, B25, B34) and South Yellow Sea (St.s H07, H09,
133 H10, H18, H19, H26, H28, H33, H35, H38) were associated accordingly in summer. In
134 winter, sampling was done only in Bohai Sea (St.s B42, B45, B47, B62, B68, BS1, BS5) and
135 North Yellow Sea (St.s B04, B08, B15, B22, B25, B33), except SYS.

136 **2.2 Sample collection**

137 Sample collection was done by multiple rosette (with CTD sensors) for different
138 depths at each sampler stations based on bottom depth. Each station was designed with three
139 distinguishing depths for better graphical analysis. Samples were collected to determine
140 phytoplankton composition, chl-a concentration, TEP abundances and its sinking rates
141 nutrients separately. Due to shallow water, depths were limited in each station between 0-100
142 meters. In 1L sampling bottle, phytoplankton samples were collected with 5% formaldehyde
143 concentration for further analysis (Guo and Sun 2018). For Chl-a analysis (Chl-a S), gathered
144 sea water of each sampling depths was filtered through 25 mm GF/F and stored in -20 °C. Sea
145 water were collected in 100ml sample bottle from all sampling depths and stored at -25°C for
146 nutrient analysis of each station. CTD sensors recorded temperature and salinity was
147 determined while sampling from different depths from study area.

148 **2.3 Biological parameters**

149 According to Welschmeyer (1994), chlorophyll – a (chl a) were measured after
150 filtering seawaters from all stations by 25 mm GF filters. Chl a concentration in samples
151 determined after were filtered onto 25 mm GF/F filters (Whatman™) and then reserved at -
152 20°C in the dark until analysis. 90% acetone were used for extraction of chl-a for 24 h at -
153 20°C in the dark, and samples were then analyzed by a laboratory fluorometer called Turner-
154 Designs Trilogy™. Phytoplankton sample (1 Liter, preserved with 30% formaldehyde) were
155 analyzed according to modified Utermöhl methods followed by Sun et al. (2002) after
156 arranging the samples (25 ml) in Utermöhl counting chamber (being settled for 24 hrs.) in
157 inverted microscope.

158 **2.4 Chemical analysis**



159 Nutrients i.e. dissolve inorganic phosphate (DIP), dissolve inorganic nitrogen (DIN),
160 dissolve silicates (DSi), ammonium, nitrate & nitrite analysis were measured by fully
161 automated (SANPLUS, Dutch SKALAR company) wet chemical analyzer (Liu et al., 2015a).
162 Measurement of TEP were sextuplicate for all samples from sampling depths by following
163 colorimetric method of Passow and Alldredge (1995) after confirming xanthan gum curve by
164 absorption measurement. At least 50ml (V_f) sample sea water were thoroughly filtered (4-6
165 replicates) at low and fixed vacuum (150 mm of Hg) through polycarbonate filters (0.4- μ m
166 pore-size) and dye binding particles on the filter for approximate 2 seconds with 500 micro
167 liters of 0.02% alcian blue (8GX; aqueous solution) in 0.06% acetic acid (pH 2.5). After
168 staining, filters are rinsed carefully with distilled water to prevent excess dye once. Dye
169 bound to substrates will not wash off by this rinsing. Filters are then soaked into 25-ml
170 beakers with 6 ml of 80% H_2SO_2 and kept for 2 hours. The beakers should be gently shaken
171 for 3-5 times during soaking period. Maximum absorption of the solution (E_{787}) lies at 787
172 nm and it was measured (μ g Xeq L^{-1}) in a 1-cm cuvette (B_{787}) against distilled water as a
173 reference. The equation is:

$$174 \quad CTEP = (E_{787} - B_{787}) \times (V_f)^{-1} \times f_x$$

175 Where, f_x =Average calibration factor and it was 9.83 μ g from the graph of xanthan gum
176 curve.

177 2.5 Measurement of TEP sinking flux

178 TEP sinking rates were determined at each station, and the SETCOL method was used
179 to measure the sinking rates according to Bienfang (1981). For measurements, a Plexiglass
180 column (height = 0.45 m and volume = 750 ml) was filled completely with a homogeneous
181 water sample within 10 min after sampling, and a cover was then placed on the set-up. In the
182 vessel, the Plexiglass column was kept to settle undisturbed for 2-3 hours, and a
183 thermostatically controlled water bath with water jackets controlled the temperature was
184 maintained by pumping its water. The settled sample of experiment was collected in sample
185 bottles by successively draining the upper, middle, and bottom compartments of the
186 Plexiglass column via piped outlet in the wall of column. The TEP biomass was measured
187 after the settlement in the samples from all three compartments. These measurements were
188 combined to calculate the sinking rate of TEPs according to the formula:

$$189 \quad V = \frac{B_s}{B_t} \times \frac{L}{t}$$



190 where V = sinking rate; B_s = the biomass of TEP settled into the bottom compartment; B_t =
191 the total biomass of TEPs in the column; L = length of the column; and t = settling interval.
192 Samples from all depths were triplicated during measurement for better data analysis and
193 marked according to stations about sinking rate as well as TEP concentrations.

194 2.6 Data analysis

195 Study stations in the map during autumn 2014 (Fig. 1A) and summer 2015 (Fig. 1b)
196 were sectioned in three vertical view for better understanding of the sample concentrations.
197 Stations in the map of winter 2015 (Fig. 1C) was divided according to seas (Fig. 1D).
198 Seasonal currents flow maps (Fig. 2) were built on the basis of secondary data and previous
199 literatures (Hwang et al. 2014; Su 1998; Yuan et al. 2008; Isobe 2008) from that area.
200 Analysis and discussions were forwarded according to both seasonal (autumn, summer &
201 winter) and oceanic (Bohai Sea, North Yellow Sea & South Yellow Sea) categories (Table 1).
202 Calculation of TEP-carbon (TEP-C, $\mu\text{g C L}^{-1}$) was determined with the slope (0.75) from the
203 equation as follows (Engel & Passow 2001):

$$204 \quad \text{TEP-C} = 0.75 \times \text{TEP}_{\text{color}} \quad (\text{Guo \& Sun 2018})$$

205 where $\text{TEP}_{\text{color}}$ is the TEP concentration (CTEP) with the unit of $\mu\text{g Xeq L}^{-1}$.

206 Various multivariate analyses were performed by using Multi Biplots software (Vicente
207 Villardón, 2015) on recorded data. Single cluster analysis was performed by Multivariate
208 Statistical Package Software with Baroni-Urbani Buser Coefficient. Linear regression,
209 Pearson correlation and covariance were performed by Microsoft Excel 2016 software.
210 Canonical correspondence analysis (CCA) were done by Canoco software, version 4.14
211 (CANOCO for Windows; Ter Braak & Šmilauer, 2002). Dominance index was used to
212 describe phytoplankton dominant species under this equation:

$$213 \quad Y = \frac{n_i}{N} \times f_i$$

214 Where, N is the total cell abundance of all species, n_i is total cell of species i and f_i is the
215 count of occurrence of species i in all sample (Guo et al. 2014). For integrated surface view
216 of recorded and examined parameters during winter 2015, Surfer 12 was used. Box-whisker
217 plots by Microsoft Excel 2016 showed the range of all recorded parameters after integration.
218 Concentrations of different parameters were graphically presented by Ocean Data View
219 (ODV 2016) software.



220

221 **3 Results**

222 **3.1 Environmental Hydrology**

223 The Bohai Sea and Yellow Sea had a complex dynamic environment with various
 224 seasonal and local geophysical currents (**Fig. 2**). Average concentration of all parameters
 225 through every season showed high chl-*a* concentration along coastal zones of BS and NYS.
 226 Average annual CTEP was higher at BS along BSCC, at NYS along YSCC and at SYS along
 227 CDW. Average annual nutrients were highly concentrated at BS than other seas, except
 228 nitrite at YSCC of SYS (Table 1).

229 During autumn 2014 (Fig. 2C), CTEP was higher at the north of NYS along LCC and
 230 CWC of southern SYS. Temperature were higher at YSCC of SYS and salinity were dense at
 231 KCC of NYS and SYS with high Chl-*a* was at LCC of NYS. Concentrations of nutrients
 232 were higher at BS except nitrite. Nitrite was higher at LCC of NYS and at YSCC of SYS.
 233 DIP, DIN, DSi and nitrate were higher at the southern part of SYS through whole autumn
 234 (Table 1).

235 During summer 2015 (Fig. 2A), CTEP was higher at southern SYS (Fig 3) with high
 236 temperature and nutrients (DIP, DIN, DSi and nitrates). Notably, DIP found high at CWC of
 237 SYS. In BS, nitrate and nitrite were higher at south coast and ammonium was higher at north-
 238 west coast with high temperature. Salinity was aggregated at KCC of NYS and mid SYS.
 239 Chl-*a* was dense at YSCC of NYS and CDW of SYS (Table 1).

240 During winter (Fig. 2B), CTEP was dense at KCC of NYS with high temperature and
 241 salinity. However, chl-*a* was higher at the north coast and BSCC of BS with YSCC of NYS
 242 too. Most of the nutrients were higher at BSCC of BS except DIP. DIP found higher at the
 243 transitional zone of BS and NYS. DSi concentration was also higher at KCC of NYS.

244 **3.1.1 Vertical concentrations in autumn 2014**

245 Vertical profile showed higher concentration of CTEP at SYS with high temperature
 246 too, especially at St. H33, H35 and H40. Chl-*a* was dense in NYS (St. B15, B19 and B25)
 247 where DSi was dramatically low. Nutrients i.e. DIN, nitrate and ammonium were found
 248 higher at the bottom of BS, especially at St. B45, B49 and B57. Salinity was lower at surface
 249 of whole study area. DIP found lowest at surface stations i.e. H07 and H09 of SYS but



highest at bottom of B34 and H07 stations. Nitrite was found higher at the SCM of NYS and SYS (Table 1). During autumn, dominant phytoplankton were *Paraliasulcate*, *Coscinodiscus* sp., *Ceratiumfusius*, *Thalassiosira* sp., *Probosica alata f. indica*, *Ceratiumtripos*, *Nitzschia* sp., *Thalassiosira pacifica*, *Guinardia delicatula* and *Thalassiosira excentrica* sequentially.

3.1.2 Vertical concentrations in summer 2015

With obvious high temperature, summer possessed low CTEP at surface of BS. CTEP was higher with low nutrients and chl-a at the SCM of Station B45. DIN, nitrate and nitrite were high near station B68. DIP and DSi were higher at the bottom of Station B57 in BS. CTEP was comparatively low at NYS with high chl-a at SCM and bottom of Station B25. DIP, DSi and nitrate were higher at the bottom of Stations B04 and B11. *Alexandrium tamarense*, *Rhizosolenia styliformis*, *Paralia sulcate*, *Guinardia flaccida*, *Dinophysis* sp., *Ceratium fusus*, *Thalassiosira excentrica*, *Ceratium furca*, *Dictyocha fibula* and *Diploneis bombus* were dominant phytoplankton accordingly through study area in summer. In SYS, CTEP was higher at the SCM with low nutrients and chl-a as BS. Nutrients along with salinity were higher at the bottom of Station H-7 and H09.

3.1.3 Vertical concentrations in winter 2015

In winter, NYS showed higher abundances of Chl-a and salinity at the stations (B04, B25 & BS5) near YSCC. Higher CTEP was found at SCM of NYS than BS. Temperature was recorded lowest in BS than NYS (**Fig. 1**), especially near shore area. Phytoplankton i.e. *Paralia sulcate*, *Thalassiosira excentrica*, *Actinopterychus* sp., *Donkinia recta*, *Thalassiosira* sp., *Coscinodiscus* sp., *Coscinodiscus subtilis*, *Navicula* sp., *Pleurosigma pelagicum* and *Coscinodiscus radiatus* were dominant during winter. Nutrients i.e., DIN, DSi, ammonium, nitrate and nitrite found higher at the SCM of Bohai Sea. DIP was found abundance in surface area at the transitional area (near Station B33) of BS and NYS (Table 1). Average nutrients were higher in BS than NYS during winter 2015. Stations near coastal area of BS (B45 & B68) and NYS (B04, B25 & BS5) have higher nutrients comparatively.

3.2 Seasonal and regional TEP concentration

Present study measured $2.13 \mu\text{g Xeq. L}^{-1}$ as average TEP concentration (CTEP) which is ranged between $0.2\text{--}23.20 \mu\text{g Xeq. L}^{-1}$. NYS ($2.32 \mu\text{g Xeq. L}^{-1}$) has more TEP concentration in average than SYS ($1.18 \mu\text{g Xeq. L}^{-1}$) and BS ($2.08 \mu\text{g Xeq. L}^{-1}$). Apparently, winter season ($6.17 \mu\text{g Xeq. L}^{-1}$) shows higher average concentration of TEP in each sea



(Table 2) than in summer ($1.10 \mu\text{g Xeq. L}^{-1}$) and in autumn ($0.67 \mu\text{g Xeq. L}^{-1}$). SYS showed higher CTEP in autumn ($0.93 \mu\text{g Xeq. L}^{-1}$) and in summer ($1.42 \mu\text{g Xeq. L}^{-1}$) than NYS and BS.

3.3 TEP associated carbon abundances

The carbon (TEP-C) associated with TEP picked at winter 2015 and became lower during autumn 2014. BS showed low carbon abundance at surface during summer (Fig. 4E). NYS possessed high TEP-C in SCM during winter (Fig. 4J) and at bottom during autumn and summer (Fig. 4B & 4F). Surface of SYS recorded high TEP-C than BS and NYS during summer (Fig. 4G). However, SYS also possessed comparatively high verity of TEP-C than BS and NYS at its SCM during autumn and summer (Fig. 4D & 4H). Average TEP-C showed high variation at SCM through study areas (Fig. 4L).

Average TEP-C was $1.47 \mu\text{g C L}^{-1}$ with seasonal highest $4.44 \mu\text{g C L}^{-1}$ during winter specially in NYS ($5.25 \mu\text{g C L}^{-1}$). SYS has higher TEP-C during autumn ($0.58 \mu\text{g C L}^{-1}$) and summer ($1.07 \mu\text{g C L}^{-1}$) than other seas. Highest TEP-C was found at SML of stations B15 ($15.78 \mu\text{g C L}^{-1}$), B22 ($17.40 \mu\text{g C L}^{-1}$) and B33 ($10.91 \mu\text{g C L}^{-1}$) of NYS during winter which showed close cluster during analysis.

3.4 Seasonal and regional TEP sedimentation

Sedimentation or sinking rates of TEP was recorded 1.03 mD^{-1} in average of all seasons (Table 3) at study area. TEP sinking rate was higher in summer (1.04 mD^{-1}) than autumn (1.02 mD^{-1}) and winter (1.03 mD^{-1}). However, winter showed high sinking rates (1.02 mD^{-1}) in BS than its summer (1.01 mD^{-1}) and autumn (0.9 mD^{-1}) data. On the other hand, comparatively high sinking rates were measured in SYS during autumn (1.13 mD^{-1}) than its summer (1.05 mD^{-1}). SYS also possessed average high sinking rates of TEP (1.09 mD^{-1}) than BS (0.9 mD^{-1}) and NYS (1.03 mD^{-1}).

3.5 TEP sinking in segmented depths

Average TEP sinking dynamics were similarly close in average at each depth (Fig. 5K). In BS, high sedimentation variation was observed at mid layer (Fig. 5A) during autumn ($0.72\text{-}1.16 \text{ mD}^{-1}$) and at surface (Fig. 5E,5I) during summer ($0.86\text{-}1.57 \text{ mD}^{-1}$) and winter ($0.64\text{-}2.06 \text{ mD}^{-1}$). Surface of NYS (Fig. 5B) has diverse sinking rates during summer ($0.77\text{-}2.47 \text{ mD}^{-1}$), mid layer (Fig. 5F) in winter ($0.72\text{-}1.53 \text{ mD}^{-1}$) and bottom (Fig. 5J) in autumn ($0.76\text{-}1.19 \text{ mD}^{-1}$). Surface of SYS (Fig. 5C) during summer ($0.62\text{-}2.40 \text{ mD}^{-1}$) and bottom



layers (Fig. 5G) during autumn ($0.78\text{--}1.55\text{ mD}^{-1}$) showed sedimentation variation accordingly. In average, bottom layer (Fig. 5D) during autumn ($0.72\text{--}1.55\text{ mD}^{-1}$) and surface of study area during summer ($0.62\text{--}2.47\text{ mD}^{-1}$) and winter ($0.64\text{--}2.06\text{ mD}^{-1}$) possessed high sinking dynamicity (Fig. 5D, 5H & 5L).

3.6 Correspondence relationships of TEP

TEP showed close correspondent relationship with DIP and chl-*a* in average (Fig. 6I) and in winter at BS (Fig. 6F) after applying CCA. However, winter at NYS showed TEP was correlated with nitrate through each station. In autumn, TEP showed average close correspondence with nitrite in CCA across study areas (Fig. 6A, 16D, 16G & 16J). During summer, TEP was averagely compliance with nitrite (Fig. 6D) through all seas (Fig. 6H and 12I) except at BS (nitrate; Fig. 6E). In average, TEP showed close correspondences with *T. excentrica* and *P. sulcata* during autumn, *R. styliformis* in summer and *P. sulcata* and *Actinoptychus* sp. were dominant across study area. Both in BS and NYS, *P. sulcata* was highly dominant and mostly correlates with concentration of TEP through all seasons. In SYS, correspondences of dominant phytoplankton with TEP were observed rather than nutrients (Fig. 6J & 6K).

Considering all parameters, most of the SYS stations clustered closely in dendrogram (Group 1 and 4) after applying Baroni-Urbani Buser coefficient during autumn (Fig. 13A) and summer (Fig. 13B). In BS, St. B45 clustered in same group with B68 through all season (autumn; group 2, summer; Group 5 and winter; Group 7). St. B15 of NYS showed group correspondence with St. B25 during autumn (Fig. 13A; Group 2) and winter (Fig. 13C; Group 8) except summer. Rest of the stations clustered randomly with each other due to their different gradients.

4 Discussions

4.1 Seasonal effect on TEP distribution

Study of seasonal trends on EPS (exopolymeric substances; equivalent to TEP) confirmed the formation of EPS at earlier season in upper sea column with time (Riedel et al. 2006, Collins et al. 2008). Traditionally, the resource of TEP and their precursors are phytoplankton cells, especially under bloom situations (Hong et al. 1997; Passow 2002a; Passow and Alldredge 1994). In BS, *Skeletonema costatum* and *Coscinodiscus oculus-iridis* during winter. *Noctiluca scintillans*, *Chaetoceros affinis*, *Chaetoceros* sp. through all seasons



343 were reported as dominant phytoplankton species (Yang et al. 2018) which may have local
344 influence on CTEP (Passow 2002a). However, *P. sulcata* showed dominance in BS through 3
345 seasons BS by corresponding closely with TEP (Fig. 6D, 6E & 6F). During autumn at NYS,
346 *Pseudo-nitzschia pungens* and *Proboscia alata* were reported dominant at the same location
347 of dense CTEP compared to present study (Li et al. 2017) which may also liable for CTEP
348 assemblages by demonstration close relation in CCA (Fig. 6G). In SYS, dominance of
349 *Paralia sulcata* and *Thalassiosira angulata* (Li et al. 2017, Liu et al. 2015a) with *Pseudo-*
350 *nitzschia pungen* (Li et al. 2017) were reported at same magnitudes during autumn which
351 were similar to present study and also maintained close correspondences with TEP (Fig. 6J).
352 Coastal SYS showed the dominance of *Skeletonema costatum* and *Thalassiosira*
353 *nordenskioeldii* during winter (Wen et al. 2007). Among phytoplankton, cyanobacteria (36%)
354 were reported stratified during summer at SYS (Liu et al. 2015b). Phytoplankton i.e. *Paralia*
355 *sulcata*, *Prorocentrum dentatum* and *Thalassiosira angulata* were abundant species at south
356 of SYS which location were highly concentrated with TEP (**Fig. 5A**) according to present
357 study. Biological process of these species may liable for the abundance of TEP along with
358 those study areas.

359 However, CTEP can be high in lower biological activity. In absence of
360 phytoplankton, dissolve organic matter can be source of TEP (Wurl et al. 2011b). During
361 autumn and summer, CTEP was abundant in this study in where nutrients were higher and
362 Chl-a was low. Arctic autumn showed low TEP concentrations in upper water layer with no
363 significant enrichment (Wurl et al. 2011). Though, limited sampling data showed no
364 significant correlation of TEP with nutrients and salinity in Changjinag (Yangtze River)
365 estuary (CE) near East China Sea (Guo & Sun 2018). However, CTEP was higher along
366 CDW from CE during this study at summer. Consumption by various organisms (Tranvik et
367 al. 1993) can also change TEP distribution. In some places during summer and autumn, due
368 to low nutrient concentration, organisms (**Fig3**) may feed on TEPs which is why CTEP (**Fig.**
369 **3**) is very low in those areas. Higher tempered zone also possessed high TEP production due
370 to the effect of temperature on photosynthetic parameters (Claquin et al. 2008, Fukao et al.
371 2012). So, CTEP has been observed high during summer and spring than other seasons in
372 various estuaries and seas (Table 8). In SYS, CTEP was higher in subsurface area with low
373 Chl-a (**Fig. 3E**) but high Temperature (**Table 1**) at YSCC and CDW during summer 2015.
374 However, changes in CTEP through seas result from a balance between sources i.e.
375 production by algae, bacteria, and possibly other organisms (Ortega-Retuerta et al. 2010)



376 which supported the present data during winter in study areas. Arctic winter season also
 377 showed the highest water column TEP concentrations and formation rates until spring (Wurl
 378 et al. 2011b). On the other hand, CTEP in spring was lower in Changjinag (Yangtze River)
 379 estuary near East China Sea than in summer (Guo & Sun 2018).

380 Studies (Table 4) showed that highest CTEP was found at the surface water column in
 381 Adriatic Sea (Radic et al. 2005) and lowest in Weddell Sea (Ortega-Retuerta et al. 2009). In
 382 North Pacific Ocean, surface possessed higher CTEP than below 50 meters (Table 5).
 383 Average CTEP was higher (Table 4) in western subarctic part (Ramaiah et al. 2005) than
 384 eastern (Wurl et al. 2011b) and western tropical parts (Kodama et al. 2014) as well as eastern
 385 subarctic zone (Wurl et al. 2011b). Higher estuarine CTEP was found in Changjinag River
 386 Estuary (Guo & Sun 2018) during both in summer and spring rather than that of Jiulong
 387 River estuary (Peng and Huang 2007) and Pearl River estuary (Sun et al. 2010). In the surface
 388 of Bay areas, present study observed lower average CTEP in Bohai Sea than in Chesapeake
 389 Bay (Malpezzi et al. 2013) and Gulf of Cadiz (Garc et al. 2002). Gulf of Aqaba showed
 390 highest CTEP (Bar-Zeev et al. 2009) below 50 meters of any seas (Table 5). Below 100m,
 391 CTEP was higher in Eastern Mediterranean Sea (Bar-Zeev et al. 2011) than other part of this
 392 sea (Ortega-Retuerta et al. 2010) and Gulf of Aqaba (Bar-Zeev et al. 2009). Average vertical
 393 CTEP profiling (0-100m) was higher in Ross Sea (Hong et al. 1997) than rest seas (Table 6).
 394 Rather than in summer 2015 and autumn 2014, Present study observed high CTEP at BSCC
 395 in Bohai Sea as well as at LCC in NYS in winter 2015. Combined effects of seasonal
 396 environmental parameters may cause these variations through those water columns.

397 **4.2 Seasonal sinking rate variations of TEP**

398 Sinking rates or particle sedimentation of TEP can also cause changes in TEP
 399 distribution (Passow et al. 2001). SETCOL method was most popular scientific method
 400 (Table 7) to track it (Guo & Sun 2018) due to its simplicity and reliability. However, motion
 401 and turbulence of seawater was ignored in SETCOL which have complex effect on particle
 402 sinking in ocean (Javier et al. 1996, Ruiz et al. 2004). So, the actual situation remained
 403 unclear with theories (Guo & Sun 2018). Seawater is denser than TEP (density 0.70-0.84 g
 404 cm⁻³) which indicated that pure TEP will ascend upward in ballast free condition (Azetsu-
 405 Scott and Passow 2004). So, sinking rates of TEP can be negative (Azetsu-Scott and Passow
 406 2004, Mari 2008). In real scenario, presence of organic and inorganic matter in seawater
 407 make complex situation for TEP to be pure. Sticky gel characteristics of TEP (Engel 2000,



408 Rochelle-Newall et al. 2010) may aggregated them with various detritus, particles and
 409 organisms i.e. bacteria, phytoplankton and mineral clays (Prieto et al. 2002) which may
 410 influence them to sink downward in water (Mari et al. 2017).

411 Freshwater lake has lower particle concentration with higher sinking rates of TEP
 412 (Table 7) due to the influence of phytoplankton cells aggregation (Vicente et al. 2009).
 413 Estuarine TEP sedimentation rate was reported lower in spring than other seasons (Guo &
 414 Sun 2018). Average sinking rate of TEP in NYS (Table 9) was observed higher in summer
 415 and winter during present study may be due to higher salinity (**Table 1**) and primary
 416 productivity (Chl-a). In SYS, highest TEP sedimentation was at Station H38 (2.40 mD^{-1}) may
 417 be caused by counter effect of CDW and CWC (**Fig. 2**). SYS also has higher sinking rates of
 418 TEP in autumn than BS and NYS may be due to high nutrient concentrations (**Fig. 4**) at the
 419 bottom that may stick with TEP to sink downwards. Rather than other coastal water
 420 (Changjiang Estuary), Bohai Sea possessed higher sinking rates of TEP in average, especially
 421 during summer (Table 9). Seasonal effect on concentrations of environmental parameters and
 422 coastal currents' activity may cause these differences in sedimentation rates of TEP in study
 423 areas.

424 **4.3 Potential role of seasonal carbon export associated with TEP**

425 Organic carbon formation in sea surface associated with TEP and its sedimentation is
 426 a complex part of carbon cycle in ocean (Mari et al. 2017). These exopolymer particles
 427 contained carbon complex which may disappeared due to TEP sedimentation and degradation
 428 by bacteria (Prieto et al. 2006) in euphotic zone. Due to alignment of TEP as same magnitude
 429 of phytoplankton cells abundance (Passow 2002b, Passow et al. 2001), TEP sinking was
 430 accepted as important carbon pathway for its dominant effect on TEP-C (Stoderegger and
 431 Herndl 1999, Obernosterer and Herndl 1995, Guo & Sun 2018). Stickiness of TEP and its
 432 balances between production and degradation rates contributed in POC cycling (Mari et al.
 433 2017) in the ocean. TEP sedimentation roughly contributes 30% in POC flux at Santa
 434 Barbara Channel (Passow et al. 2001) and 0.02%-31% in oligotrophic reservoir of southern
 435 Spain (Mari et al. 2017). TEP-C was lower in spring than in summer at Changjiang River
 436 (Yangtze River) estuary near East China Sea. Present study observed higher total average of
 437 TEP-C in NYS than BS and SYS especially in winter and lowest TEP-C in autumn in BS
 438 during all three seasons. Considering the complex effect of all environmental parameters,
 439 TEP-C distribution showed similar correlations with nutrients and Chl-a as CTEP in different



seasons accordingly. Results of present study suggest the importance of TEP in POC cycle in Bohai Sea and Yellow Sea compared to phytoplankton cells and zooplankton fecal pellets (Turner 2002, Turner 2015). TEP controlled the biological carbon pump of atmospheric CO₂ (Mari et al. 2017). With significant seasonal TEP-C distribution, the data showed an unavoidable importance of TEP and its sedimentation rates for exporting carbon in study areas.

5 Conclusions

Seasonal variations of TEP concentration was complex and mostly depends on nutrients and Chl-a. Correlations on the basis of 168 samples of TEP with same amount of other environmental parameters showed variations among seas as well as seasons. Temperature varied from 0-28 °C round the year but TEP stacked from 0 to below 10 µg Xeq. L⁻¹ in average. Chl-a may liable for TEP distribution during autumn and summer, especially in SYS and nutrients to TEP in winter in BS. Coastal current mixing has an influence on CTEP due to its dominancy at dilution zones. Sinking rates of TEP mostly varied at surface of BS and NYS during summer and winter. SYS has moderated sinking rates of TEP at its surface and bottom with higher nutrients concentrations. With close correspondences, dominant phytoplankton i.e. *P. sulcata*, *T. excentrica* and *R. styliformis* have influences of high TEP concentration. Average carbon exports maintained same magnitudes with TEP during each season. Average TEP sinking was diverse at SCM but higher at surface through all seasons. Further research on POC cycle by measuring CTEP, TEP-C and its sinking rates with seawater density and turbidity of selected study area are recommended to be more precise on carbon contributions of exopolymers in the process of biological and chemical carbon pump in open and coastal seas.

Acknowledgements

This study was supported by National Natural Science Foundation of China (Nos. 41876134, 41676112 and 41276124), the Key Project of Natural Science Foundation for Tianjin (No. 17JCZDJC40000), the University Innovation Team Training Program for Tianjin (TD12-5003) and the Tianjin 131 Innovation Team Program (20180314), and the Changjiang Scholar Program of Chinese Ministry of Education to Jun Sun. The authors are grateful to Prof. Houjie Wang for providing the data of temperature and salinity, and also thank the crew and captain of the R/V Dongfanghong 2 for their assistance in sample



471 collection during the cruise supported by National Natural Science Foundation of China
 472 (Nos. NORC2014 and NORC2015).

473 References

474 Alldredge, A.L., Passow, U., and Logan, B.E.: The abundance and significance of a class
 475 of large, transparent organic particles in the ocean. *Deep-Sea Res. I Oceanogr.*
 476 *Res. Pap.* 40. [http://dx.doi.org/10.1016/0967-0637\(93\)90129-Q](http://dx.doi.org/10.1016/0967-0637(93)90129-Q), 1993.

477 Aller, J.Y., Kuznetsova, M.R., Jahns, C.J., and Kemp, P.F.: The sea surface microlayer as
 478 a source of viral and bacterial enrichment in marine aerosols. *J. Aerosol Sci.*
 479 36: 801–812. <http://dx.doi.org/10.1016/j.jaerosci.2004.10.012>, 2005.

480 Azetsu-Scott K. : Ascending marine particles : significance of transparent exopolymer
 481 particles (TEP) in the upper ocean[J]. *Limnology and Oceanography*, 49 (3
 482) : 741-748, 2004.

483 Azetsu-Scott, K., and Passow, U. : Ascending marine particles: significance of transparent
 484 exopolymer particles (TEP) in the upper ocean. *Limnol. Oceanogr.* 49:741–
 485 748. <http://dx.doi.org/10.4319/lo.2004.49.3.0741>, 2004.

486 Bar-Zeev, E., and Rahav, E. : Microbial metabolism of transparent exopolymer particles
 487 during the summer months along a eutrophic estuary system. *Front. Microbiol.*
 488 6: 403. <http://dx.doi.org/10.3389/fmicb.2015.00403>, 2015.

489 Bar-Zeev, E.; Berman-Frank, I.; Stambler, N.; Vazquez Domínguez, E.; Zohary, T.;
 490 Capuzzo, E.; Meeder, E.; Suggett, D.; Iluz, D.; Dishon, G.; et al. Transparent
 491 exopolymer particles (TEP) link phytoplankton and bacterial production in the
 492 Gulf of Aqaba. *Aquat. Microb. Ecol.* 56, 217–225, 2009.

493 Bar-Zeev, E., Berman, T., Rahav, E., Dishon, G., Herut, B., Kress, N., and Berman-
 494 Frank, I. : Transparent exopolymer particle (TEP) dynamics in the eastern
 495 Mediterranean Sea. *Mar Ecol Prog Ser* 431: 107–118, 2011.

496 Bienfang, P.K.: SETCOL— a technologically simple and reliable method for measuring
 497 phytoplankton sinking rates. *Canadian Journal of Fisheries and Aquatic*
 498 *Sciences*. 38(10): 1289-1294. <https://doi.org/10.1139/f81-173>, 1981.



- 499 Bigg, E.K., and Leck, C. :The composition of fragments of bubbles bursting at the ocean
500 surface. J. Geophys. Res. 113, D11209.
501 <http://dx.doi.org/10.1029/2007JD009078>, 2008.
- 502 Burd, A., Buchan, A., Church, M.J., Landry, M.R., McDonnell, A.M.P., Passow, U.,
503 Steinberg, D.K., and Benway, H.M. : Towards a transformative understanding
504 of the ocean's biological pump: priorities for future research. Report on the
505 NSF Biology of the Biological Pump Workshop. Ocean Carbon and
506 Biogeochemistry (OCB) Program, Woods Hole, MA
507 <http://dx.doi.org/10.1575/1912/8263>, 2016.
- 508 Burd, A.B., and Jackson, G.A. :Particle aggregation. Annu. Rev. Mar. Sci. 1:65–90.
509 [http:// dx.doi.org/10.1146/annurev.marine.010908.163904](http://dx.doi.org/10.1146/annurev.marine.010908.163904), 2009.
- 510 Claquin, P., Probert, I., Lefebvre, S., and Veron, B. :Effects of temperature on
511 photosynthetic parameters and TEP production in eight species of marine
512 microalgae. Aquat. Microb. Ecol. 51:1–11.
513 <http://dx.doi.org/10.3354/ame01187>, 2008.
- 514 Corzo A, Rodriguez-Galvez, S., Lubian, L., Sangrá, P., Martínez, A., and Morillo, J.A. :
515 Spatial distribution of transparent exopolymer particles in the Bransfield
516 Strait, Antarctica. Journal of Plankton Research. 27(7): 635–646.
517 <https://doi.org/10.1093/plankt/fbi038>, 2005.
- 518 Corzo, A., Morillo, J.A. and Rodríguez, S. : Production of transparent exopolymer
519 particles (TEP) in cultures of *Chaetoceros calcitrans* under nitrogen limitation.
520 Aquat. Microb. Ecol. 23, 63–72, 2000.
- 521 Cunliffe, M., Engel, A., Frka, S., Gašparović, B., Guitart, C., Murrell, J.C., Salter, M.,
522 Stolle, C., Upstill-Goddard, R., and Wurl, O. : Sea surface microlayers: a
523 unified physicochemical and biological perspective of the air-ocean interface.
524 Prog. Oceanogr. 109: 104–116.
525 <http://dx.doi.org/10.1016/j.pocean.2012.08.004>, 2013.
- 526 DeMott, P.J., Hill, T.C.J., McCluskey, C.S., Prather, K.A., Collins, D.B., Sullivan,
527 R.C., Ruppel, M.J., Mason, R.H., Irish, V.E., Lee, T., Hwang, C.Y., Rhee,
528 T.S., Snider, J.R., McMeeking, G.R., Dhaniyala, S., Lewis, E.R., Wentzell,
529 J.J.B., Abbatt, J., Lee, C., Sultana, C.M., Ault, A.P., Axson, J.L., Diaz



- 530 Martinez, M., Venero, I., Santos-Figueroa, G., Stokes, M.D., Deane, G.B.,
531 Mayol-Bracero, O.L., Grassian, V.H. Bertram, T.H., Bertram, A.K., Moffett,
532 B.F. and Franc, G.D. : Sea spray aerosol as a unique source of ice nucleating
533 particles. Proc. Natl. Acad. Sci. U. S. A.
534 <http://dx.doi.org/10.1073/pnas.1514034112>, 2015.
- 535 Engel, A, and Passow, U.: Carbon and nitrogen content of transparent exopolymer
536 particles (TEP) in relation to their Alcian Blue adsorption. Marine Ecology
537 Progress Series. 2001; 219: 1-10. <https://doi.org/10.3354/meps219001>, 2001.
- 538 Engel, A.: The role of transparent exopolymer particles (TEP) in the increase in apparent
539 particle stickiness during the decline of a diatom bloom. Journal of Plankton
540 Research. 22(3): 485-497. <https://doi.org/10.1093/plankt/22.3.485>, 2000.
- 541 Engel, A.: Direct relationship between CO₂ uptake and transparent exopolymer particles
542 production in natural phytoplankton. Journal of Plankton Research. 24(1): 49-
543 53. <https://doi.org/10.1093/plankt/24.1.49>, 2002.
- 544 Engel, A.: Distribution of transparent exopolymer particles (TEP) in the northeast
545 Atlantic Ocean and their potential significance for aggregation processes.
546 Deep Sea Research I. 51(1): 83-92. <https://doi.org/10.1016/j.dsr.2003.09.001>,
547 2004.
- 548 Fu, M.Z., Wang, Z.L., Li, Y., Li, R.X., Sun, P., Wei, X.H., Lin, X.Z., and Guo, J.S.:
549 Phytoplankton biomass size structure and its regulation in the Southern
550 Yellow Sea (China): seasonal variability. Cont. Shelf Res. 29 2178–2194,
551 2009.
- 552 Fukao, T, Kimoto, K., and Kotani, Y.: Effect of temperature on cell growth and
553 production of transparent exopolymer particles by the diatom *Coscinodiscus*
554 *granii* isolated from marine mucilage. Journal of Applied Phycology. 24: 181-
555 186. <https://doi.org/10.1007/s10811-011-9666-3>, 2012.
- 556 Garc, C., Prieto, L., Vargas, M., et al. Hydrodynamics and the spatial distribution of
557 plankton and TEP in the Gulf of Cádiz (SW Iberian Peninsula), Journal of
558 Plankton Research 24 : 817-833, 2002.



- 559 Guo, S., and Sun, X.: Carbon biomass, production rates and export flux of copepods fecal
560 pellets in the Changjiang (Yangtze) River estuary. *Journal of Oceanology and*
561 *Limnology*, 36(4), 1244–1254. doi:10.1007/s00343-018-7057-1, 2018.
- 562 Hong Y, Smith, W.O., and White, A.M.: Studies on transparent exopolymer particles
563 (TEP) produced in the Ross Sea (Antarctica) and by *Phaeocystis antarctica*
564 (*Prymnesiophyceae*). *J Phycol.* 33:368–376, 1997.
- 565 Huang, C. J., Dong, Q.X., and Lin J.D.: Impact of global change on marine fisheries and
566 adaptation options. *Journal of Oceanography in Taiwan Strait*, 18(4): 481-494,
567 1999. (in Chinese with English abstract)
- 568 Hwang, J.H., Van, S. P., Choi, B.-J., Chang, Y. S., and Kim, Y. H.: The Physical
569 Processes in the Yellow Sea, *Ocean & Coastal Management*, 102 (2014), 449-
570 57, 2014.
- 571 Isobe, A.: Recent advances in ocean-circulation research on the Yellow Sea and East
572 China Sea shelves. *J. Oceanogr.* 64, 569e584, 2008.
- 573 Iversen, M.H., and Robert, M.L.: Ballasting effects of smectite on aggregate formation
574 and export from a natural plankton community. *Mar. Chem.* 175:18–27.
575 <http://dx.doi.org/10.1016/j.marchem.2015.04.009>, 2015.
- 576 Javier, R., Carlos, M.G., and Jaime, R.: Sedimentation loss of phytoplankton cells from
577 the mixed layer: effects of turbulence levels. *Journal of Plankton Research*.
578 18(9): 1727-1734. <https://doi.org/10.1093/plankt/18.9.1727>, 1996.
- 579 Jokulsdottir, T., and Archer D.: A stochastic, Lagrangian model of sinking biogenic
580 aggregates in the ocean (SLAMS 1.0): model formulation, validation and
581 sensitivity. *Geosci. Model Dev.* 9. [http://dx.doi.org/10.5194/gmd-9-1455-](http://dx.doi.org/10.5194/gmd-9-1455-2016)
582 2016, 2016.
- 583 Kodama T., Kurogi, H., Okazaki, M., Jinbo, T., and others.: Vertical distribution of
584 transparent exopolymer particle (TEP) concentration in the oligotrophic
585 western tropical North Pacific. *Mar Ecol Prog Ser* 513:29-37.
586 <https://doi.org/10.3354/meps10954>, 2014



- 587 Li, X., Feng, Y., Leng, X., Liu, H., and Sun, J.: Phytoplankton species composition of
588 four ecological provinces in Yellow Sea, China. *Journal of Ocean University*
589 of China, 16(6), 1115–1125. doi:10.1007/s11802-017-3270-3, 2017.
- 590 Lili, M. A., Chen, M., Guo, L., Lin, F., and Tong, J.: Distribution and source of
591 transparent exopolymer particles in the northern bering sea. *Acta*
592 *Oceanologica Sinica*, 34(5), 81-90, 2012.
- 593 Liu, H., Huang, Y., Zhai, W., Guo, S., Jin, H., and Sun, J.: Phytoplankton communities
594 and its controlling factors in summer and autumn in the southern Yellow Sea,
595 China. *Acta Oceanologica Sinica*, 34(2), 114–123. doi:10.1007/s13131-015-
596 0620-0, 2015a.
- 597 Liu, X., Huang, B., Huang, Q., Wang, L., Ni, X., Tang, Q., ... Sun, J.: Seasonal
598 phytoplankton response to physical processes in the southern Yellow Sea.
599 *Journal of Sea Research*, 95, 45–55. doi: 10.1016/j.seares.2014.10.017, 2015b
- 600 Logan, B.E., Passow, U., Alldredge, A.L., Grossartt, H.P., and Simont, M.: Rapid
601 formation and sedimentation of large aggregates is predictable from
602 coagulation rates (half-lives) of transparent exopolymer particles (TEP). *Deep-*
603 *Sea Res. II* 42 203–214, 1995.
- 604 Malpezzi, M.A., Sanford, L.P., and Crump, B.C.: Abundance and distribution of
605 transparent exopolymer particles in the estuarine turbidity maximum of
606 Chesapeake Bay. *Marine Ecology Progress Series*, 486 : 23-35, 2013.
- 607 Mari, X.: Does ocean acidification induce an upward flux of marine aggregates[J] ?
608 *Biogeosciences*, 5 (4) : 1023-1031, 2008.
- 609 Mari, X., Rassoulzadegan, F., Brussaard, C.R.D., and Wassmann, P.: Dynamics of
610 transparent exopolymeric particles (TEP) production by *Phaeocystis globosa*
611 under N- or P-limitation: a controlling factor of the retention/export balance.
612 *Harmful Algae* 4: 895–914. <http://dx.doi.org/10.1016/j.hal.2004.12.014>, 2005.
- 613 Mari, X., Passow, U., Migon, C., Burd, A.B., and Legendre, L.: Transparent exopolymer
614 particles: Effects on carbon cycling in the ocean. *Progress in Oceanography*,
615 151, 13–37. doi:10.1016/j.pocean.2016.11.002, 2017.



- 616 Mari, X., J.P. Torréton, C.B.T. Trinh, T. Bouvier, C.V. Thuoc, J.P. Lefebvre, and
617 S.Ouillon.: Aggregation dynamics along a salinity gradient in the Bach Dang
618 estuary, North Vietnam. *Estuarine, Coastal and Shelf Science*. 96: 151-158.
619 <https://doi.org/10.1016/j.ecss.2011.10.028>, 2012.
- 620 Mopper, K., Zhou, J., Sri Ramana, K., Passow, U., Dam, H.G., and Drapeau, D.T.: The
621 role of surface-active carbohydrates in the flocculation of a diatom bloom in a
622 mesocosm. *Deep-Sea Res. II Top. Stud. Oceanogr.* 42:47–73.
623 [http://dx.doi.org/10.1016/0967-0645\(95\)00004-A](http://dx.doi.org/10.1016/0967-0645(95)00004-A), 1995.
- 624 Mopper, K., Zhou, J., Sri Ramana, K., Passow, U., Dam, H.G., and Drapeau, D.T.: The
625 role of surface-active carbohydrates in the flocculation of a diatom bloom in a
626 mesocosm. *Deep-Sea Res. II Top. Stud. Oceanogr.* 42:47–73.
627 [http://dx.doi.org/10.1016/0967-0645\(95\)00004-A](http://dx.doi.org/10.1016/0967-0645(95)00004-A), 1995.
- 628 Naimie, C.E., Blain, C.A., and Lynch, D.R.: Seasonal mean circulation in the Yellow Sea
629 — a model-generated climatology. *Continental Shelf Research* 21(6-7), 667–
630 695. doi:10.1016/s0278-4343(00)00102-3, 2001.
- 631 Obernosterer, I., and Herndl, G.J.: Phytoplankton extracellular release and bacterial
632 growth: dependence on inorganic N: P ratio. *Marine Ecology Progress*
633 *Series*.116: 247-257. <https://doi.org/10.3354/meps116247>, 1995.
- 634 Orellana, M.V., Matrai, P.A., and Leck, C., Rauschenberg, C.D., Lee, A.M., and Coz, E.:
635 Marine microgels as a source of cloud condensation nuclei in the high arctic.
636 *Proc. Natl. Acad. Sci. U. S. A.* 108, 13612–13617, 2011.
- 637 Orellana, M.V., Matrai, P.A., Leck, C., Rauschenberg, C.D., Lee, A.M., and Coz, E.:
638 Marine microgels as a source of cloud condensation nuclei in the high arctic.
639 *Proc. Natl. Acad. Sci. U. S. A.* 108, 13612–13617, 2011.
- 640 Ortega-Retuerta, E., Duarte, C.M., and Reche, I.: Significance of Bacterial Activity for
641 the Distribution and Dynamics of Transparent Exopolymer Particles in the
642 Mediterranean Sea. *Microbial Ecology*, 59(4), 808–818. doi:10.1007/s00248-
643 010-9640-7, 2010.



- 644 Ortega-Retuerta, E., Reche, I., Pulida-Villena, E., et al.: Uncoupled distributions of
645 transparent exopolymer particles (TEP) and dissolved carbohydrates in the
646 Southern Ocean. *Marine Chemistry*, 115 : 59-65, 2009.
- 647 Passow, U.: Production of transparent exopolymer particles (TEP) by phyto- and
648 bacterioplankton. *Mar. Ecol. Prog. Ser.* 236:1–12. [http://dx.doi.org/10.3354/](http://dx.doi.org/10.3354/meps236001)
649 [meps236001](http://dx.doi.org/10.3354/meps236001), 2002a.
- 650 Passow, U.: Transparent exopolymer particles (TEP) in aquatic environments. *Prog.*
651 *Oceanogr.* 55 287–333, 2002b.
- 652 Passow, U., Alldredge, A.L., and Logan, B.E.: The role of particulate carbohydrate
653 exudates in the flocculation of diatom blooms. *Deep-Sea Res. I Oceanogr.*
654 *Res. Pap.* 41:335–357. [http://dx.doi.org/10.1016/0967-0637\(94\)90007-8](http://dx.doi.org/10.1016/0967-0637(94)90007-8),
655 1994.
- 656 Passow, U., and Alldredge, A.L.: Distribution, size and bacterial-colonization of
657 transparent exopolymer particles (Tep) in the ocean. *Mar Ecol Prog Ser*
658 113:185–198, 1994.
- 659 Passow, U., and Alldredge, A.L.: A dye-binding assay for the spectrophotometric
660 measurement of transparent exopolymer particles (TEP). *Limnol. Oceanogr.*
661 40, 1326–1335, 1995.
- 662 Passow, U., Shipe, R.F., Murray, A., Pak, D.K., Brzezinski, M.A., and Alldredge, A.L.:
663 The origin of transparent exopolymer particles (TEP) and their role in the
664 sedimentation of particulate matter. *Cont Shelf Res* 21:327–346, 2001.
- 665 Peng, A.G., and Huang, Y.P.: Study on TEP and its relationships with Uranium, Thorium,
666 Polonium Isotopes in Jiulong Estuary. *Journal of Xiamen University*. 46(1):
667 38-42, 2007. (in Chinese with English abstract)
- 668 Prairie, J.C., Ziervogel, K., Camassa, R., McLaughlin, R.M., White, B.L., Dewald, C.,
669 and Arnosti, C.: Delayed settling of marine snow: effects of density gradient
670 and particle properties and implications for carbon cycling. *Mar. Chem.*
671 175:28–38. <http://dx.doi.org/10.1016/j.marchem.2015.04.006>, 2015.
- 672 Prieto, L., Navarro, G., Cózar, A., Echevarría, F., and García, C.M.: Distribution of TEP
673 in the euphotic and upper mesopelagic zones of the southern Iberian coasts.



- 674 Deep Sea Research II. 53(11-13): 1314-1328.
675 <https://doi.org/10.1016/j.dsr2.2006.03.009>, 2006.
- 676 Prieto, L., Ruiz, J., Echevarría, F., García, C.M., Bartual, A., Gálvez, J.A., Corzo, A., and
677 Macías, D.: Scales and processes in the aggregation of diatom blooms: high
678 time resolution and wide size range records in a mesocosm study. Deep Sea
679 Research II. 49: 1233-1253. [https://doi.org/10.1016/S0967-0637\(02\)00024-9](https://doi.org/10.1016/S0967-0637(02)00024-9),
680 2002.
- 681 Quinn, P.K., Bates, T.S., Schulz, K.S., Coffman, D.J., Frossard, A.A., Russell, L.M.,
682 Keene, W.C., and Kieber, D.J.: Contribution of sea surface carbon pool to
683 organic matter enrichment in sea spray aerosol. Nat. Geosci. 7 228–232, 2014.
- 684 Radić, T., Kraus, R., Fuks, D., Radić, J., and Pečar, O.: Transparent exopolymeric
685 particles' distribution in the northern Adriatic and their relation to
686 microphytoplankton biomass and composition. Science of The Total
687 Environment, 353(1-3), 151–161. doi: 10.1016/j.scitotenv.2005.09.013, 2005.
- 688 Ramaiah, N., Takeda, S., Furuya, K., Yoshimura, T., and others.: Effect of iron
689 enrichment on the dynamics of transparent exopolymer particles in the western
690 subarctic Pacific. Prog Oceanogr 64:253–261, 2005.
- 691 Ramaiah, N., Yoshikawa, T., and Furuya, K.: Temporal variations in transparent
692 exopolymer particles (TEP) associated with a diatom spring bloom in a
693 subarctic ria in Japan. Marine Ecology Progress Series. 212: 79-88.
694 <https://doi.org/10.3354/meps212079>, 2001.
- 695 Rochelle-Newall, E.J., Mari, X., and Pringault, O.: Sticking properties of transparent
696 exopolymeric particles (TEP) during aging and biodegradation. Journal of
697 Plankton Research. 32(10): 1433-1442. <https://doi.org/10.1093/plankt/fbq060>
- 698 Ruiz, J., Macías, D., and Peters, F.: Turbulence increases the average settling velocity of
699 phytoplankton cells. Proceeding of the National Academy of Science of the
700 United States of America. 101(51): 17720-17724.
701 <https://doi.org/10.1073/pnas.0401539101>, 2004.



- 702 Stoderegger, K., and Herndl, G.J.: Production of exopolymer particles by marine
703 bacterioplankton under contrasting turbulence conditions. *Marine Ecology*
704 *Progress Series*. 189: 9-16. <https://doi.org/10.3354/meps189009>, 1999.
- 705 Su, J.: Circulation dynamics of the China seas: north of 181N. In: Robinson, A.R., Brink,
706 K., (Eds.), *The Sea*, vol. 11. *The Global Coastal Ocean: Regional Studies and*
707 *Syntheses*. Wiley, New York, pp. 483–506, 1999, 1998.
- 708 Sun, C.C., Wang, Y.S., Wu, M.L., Li, N., Lin, L., Song, H., Wang, Y.T., Deng, C., Peng,
709 Y.L., Sun, F.L., and Li, C.L.: Distribution of transparent exopolymer particles
710 in the Pearl River Estuary in summer. *Journal of Tropical Oceanography*.
711 29(5): 81-87, 2010. (in Chinese with English abstract)
- 712 Tang, Q. S., Jin, X.S., Wang, J., Zhuang, Z.M., Cui, Y., and Meng, T.X.: Decadal-scale
713 variations of ecosystem productivity and control mechanisms in the Bohai
714 Sea. *Fisheries Oceanography*, 12(4-5): 223-233, 2003.
- 715 Tang, Q.S., and Su, J. L.: *Marine Ecosystem Dynamics Study of China. Key Scientific*
716 *Questions and Developing Strategies* (in Chinese). Beijing: Science Press, 3–
717 34, 2001.
- 718 Tang, Q.S., Su, J.L., and Zhang, J.: China GLOBEC II: a case study of the Yellow Sea
719 and East China Sea ecosystem dynamics preface. *Deep-Sea Res. II* 57, 993–
720 995, 2010.
- 721 Tang, Q.S., Su, J.L., Kishi, M.J., and Oh, I.S.: An introduction to the Second China–
722 Japan– Korea Joint GLOBEC Symposium on the ecosystem structure, food
723 web trophodynamics and physical-biological processes in the Northwest
724 Pacific. *J. Mar. Syst.* 67, 203–204, 2007.
- 725 Ter-Braak, C.J.F., and Šmilauer, P.: *CANOCO Reference Manual and CanoDraw for*
726 *Windows User's Guide: Software for Canonical Community Ordination*
727 *(Version 4.5)*. Microcomputer Power, Wageningen. Soil macrofauna in
728 organic and conventional coffee plantations in Brazil, 2002.
- 729 Thuy, N.T., Lin, J.C.-T., Juang, Y., and Huang, C.: Temporal variation and interaction of
730 full size spectrum Alcan blue stainable materials and water quality parameters
731 in a reservoir. *Chemosphere* 131:139–148.
732 <http://dx.doi.org/10.1016/j.chemosphere.2015.03.023>, 2015.



- 733 Tranvik, L.J., Sherr, E.B., and Sherr, B.F.: Uptake and utilization of colloidal DOM by
734 heterotrophic flagellates in seawater. *Mar EcolProg Ser* 92:301–309, 1993.
- 735 Turner, J.T.: Zooplankton fecal pellets, marine snow and sinking phytoplankton blooms.
736 *Aquatic Microbial Ecology*. 27: 57-102. <https://doi.org/10.3354/ame027057>,
737 1993, 2002.
- 738 Turner, J.T.: Zooplankton fecal pellets, marine snow, phytodetritus and the ocean's
739 biological pump. *Progress in Oceanography*. 130: 205-248.
740 <https://doi.org/10.1016/j.pocean.2014.08.005>, 2015.
- 741 Verdugo, P., Alldredge, A.L., Azam, F., Kirchman, D.L., Passow, U., and Santschi, P.H.:
742 The oceanic gel phase: a bridge in the DOM-POM continuum. *Mar. Chem.* 92,
743 67–85, 2004.
- 744 Vicente Villardón, J.L. MULTBILOT: A package for Multivariate Analysis using
745 Biplots. Departamento de Estadística. Universidad de Salamanca, 2015.
746 (<http://biplot.usal.es/ClassicalBiplot/index.html>)
- 747 Vicente, I. D.: Retuerta E O. Contribution of transparent exopolymer particles to carbon
748 sinking flux in an oligotrophic reservoir[J]. *Biogeochemistry*, 96 : 13-23,
749 2009.
- 750 Vicente, I.D., Ortega-Retuerta, E., Romera, O., Moreles-Baquero, R., and Reche, I.:
751 Contribution of transparent exopolymer particles to carbon sinking flux in an
752 oligotrophic reservoir. *Biogeochemistry*. 96: 13-23.
753 <https://doi.org/10.1007/s10533-009-9342-8>, 2009.
- 754 Wang, X., Sultana, C.M., Trueblood, J., Hill, T.C.J., Malfatti, F., Lee, C., Laskina, O.,
755 Moore, K.A., Beall C.M., McCluskey, C.S., Cornwell, G.C., Zhou, Y., Cox,
756 J.L., Pendergraft, M.A., Santander, M.V., Bertram, T.H., Cappa, C.D., Azam,
757 F., DeMott, P.J., Grassian, V.H., and Prather, K.A.: Microbial control of sea
758 spray aerosol composition: a tale of two blooms. *ACS Cent. Sci.* 1:124–131.
759 <http://dx.doi.org/10.1021/acscentsci.5b00148>, 2015.
- 760 Welschmeyer, N. A.: Fluorometric analysis of chlorophyll-a in the presence of
761 chlorophyll-b and pheopigments [J]. *Limnology and Oceanography*, 39 :
762 1985-1992, 1994 .



- 763 Wen, L., Sun, J., He, Q., Wang, D., and Wang, M.: Winter phytoplankton assemblages of
764 coastal Yellow Sea connected to Jiaozhou Bay, China. *Journal of Ocean*
765 *University of China*, 6(1), 40–46. doi:10.1007/s11802-006-0040-7, 2007.
- 766 Wetz, M. S., Robbins, M.C., and Paerl, H.W.: Transparent exopolymer particles (TEP)
767 in a river-dominated estuary: spatial and temporal distributions and an
768 assessment of controls upon TEP formation. *Estuaries and Coasts*, 32 (3) :
769 447–455, 2009.
- 770 Wilson, T.W., Ladino, L.A., Alpert, P.A., Breckels, M.N., Brooks, I.M., Browse, J.,
771 Burrows, S.M., Carslaw, K.S., Huffman, J.A., Judd, C., Kilthau, W.P., Mason,
772 R.H., McFiggans, G., Miller, L.A., Nájera, J.J., Polishchuk, E., Rae, S.,
773 Schiller, C.L., Si, M., Temprado, J.V., Whale, T.F., Wong, J.P.S., Wurl, O.,
774 Yakobi-Hancock, J.D., Abbatt, J.P.D., Aller, J.Y., Bertram, A.K., Knopf,
775 D.A., and Murray, B.J.: A marine biogenic source of atmospheric ice-
776 nucleating particles. *Nature* 525:234–238. [http://dx.doi.org/10.](http://dx.doi.org/10.1038/nature14986)
777 1038/nature14986, 2015.
- 778 Wurl, O., and Holmes, M.: The gelatinous nature of the sea-surface microlayer. *Mar.*
779 *Chem.* 110:89–97. <http://dx.doi.org/10.1016/j.marchem.2008.02.009>, 2008.
- 780 Wurl, O., Wurl, E., Miller, L., Johnson, K., and Vagle, S.: Formation and global
781 distribution of sea-surface microlayers. *Biogeosciences* 8:121–135.
782 <http://dx.doi.org/10.5194/bg-8-121-2011>, 2011a.
- 783 Wurl, O., Miller, L., and Vagle, S.: Production and fate of transparent exopolymer
784 particles in the ocean. *J. Geophys. Res. C: Oceans* 116, 2011b.
- 785 Wurl, O., Miller, L., Röttgers, R., and Vagle, S.: The distribution and fate of surface-
786 active substances in the sea-surface microlayer and water column. *Mar. Chem.*
787 115:1–9. <http://dx.doi.org/10.1016/j.marchem.2009.04.007>, 2009.
- 788 Xu, S., Song, J., Li, X., Yuan, H., Li, N., Duan, L., and Sun, P.: Changes in nitrogen and
789 phosphorus and their effects on phytoplankton in the Bohai Sea. *Chinese*
790 *Journal of Oceanology and Limnology* 28(4), 945–952. doi:10.1007/s00343-
791 010-0005-3, 2010.



- 792 Yang, G., Wu, Z., Song, L., and Lu, X.: Seasonal Variation of Environmental Variables
793 and Phytoplankton Community Structure and Their Relationship in Liaodong
794 Bay of Bohai Sea, China. *Journal of Ocean University of China*, 17(4), 864–
795 878. doi:10.1007/s11802-018-3407-z, 2018.
- 796 Yuan, D., Zhu, J., Li, C., and Hu, D.: Cross-shelf circulation in the Yellow and East
797 China Seas indicated by MODIS satellite observations. *J. Mar. Syst.* 70
798 (2008), 134e149, 2008.
- 799 Zang, J., Tang, Y., Zou E., and Lie, H.-J.: Analysis of Yellow Sea circulation. *Chinese*
800 *Science Bulletin*, 48(S1), 12–20. doi:10.1007/bf02900935, 2003.
- 801 Zetsche, E.-M., and Ploug, H.: Marine chemistry special issue: Particles in aquatic
802 environments: From invisible exopolymers to sinking aggregates. *Mar. Chem.*
803 175, 1–4, 2015.
- 804 Zhang, F., Li, C.L., Sun, S., Wu, Y.L., and Ren, J.P.: Distribution patterns of chlorophyll
805 a in spring and autumn in association with hydrological features in the
806 southern Yellow Sea and northern East China Sea. *Chin. J. Oceanol. Limnol.*
807 27, 784–792, 2009.
- 808 Zhang, S., Leng, X., Feng, Y., Ding, C., Yang, Y., Wang, J., ... Sun, J.: Ecological
809 provinces of spring phytoplankton in the Yellow Sea: species composition.
810 *Acta Oceanologica Sinica*, 35(8), 114–125. doi:10.1007/s13131-016-0872-3,
811 2016.
- 812
- 813
- 814
- 815
- 816
- 817
- 818
- 819



Table 1 Average concentration of environmental parameters along with related seas during study seasons.

Seasons	Seas	Temperat ure (°C)	Salini ty (PSU)	DIP ($\mu\text{mol/l}$)	DIN($\mu\text{mol/l}$)	DSi($\mu\text{mol/l}$)	Ammonium($\mu\text{mol/l}$)	Nitrite($\mu\text{mol/l}$)	Nitrate($\mu\text{mol/l}$)	Chl- a($\mu\text{g/l}$)
Autumn (2014)	Bohai Sea	9.77	24.13	0.29	10.24	7.24	0.98	0.18	9.08	0.34
	North Yellow Sea	13.23	31.56	0.18	3.91	3.70	0.45	0.27	3.19	0.35
	South Yellow Sea	16.32	31.60	0.22	4.95	5.64	0.58	0.16	4.21	0.78
Summer (2015)	Bohai Sea	23.90	30.55	0.08	3.94	3.91	0.85	0.63	2.45	1.02
	North Yellow Sea	20.40	31.71	0.14	2.01	2.55	0.53	0.27	1.21	0.83
	South Yellow Sea	21.40	31.28	0.19	4.15	4.01	0.57	0.23	3.35	1.42
Winter (2015)	Bohai Sea	0.29	6.43	0.29	4.28	4.28	1.78	0.19	2.31	4.82
	North Yellow Sea	4.73	32.20	0.14	1.06	3.50	0.47	0.09	0.49	7.00



Table 2 Variations of average TEP concentrations and its sinking rates in different seas during study.

Seasons	Ranges	BS	NYS	SYS
CTEP ($\mu\text{g Xeq. L}^{-1}$)	Average	2.08	3.32	1.18
	Maximum	14.75	23.20	11.99
	Minimum	0.20	0.20	0.19
Sinking rate of TEP (m d^{-1})	Average	0.98	1.03	1.09
	Maximum	2.06	2.47	2.40
	Minimum	0.64	0.72	0.62



Table 3 Variations of average TEP concentrations and its sinking rates in different seasons.

Seasons	Ranges	Sinking rate of TEP	CTEP
		(m d ⁻¹)	(µg Xeq. L ⁻¹)
Total Average	Average	1.03	2.13
	Maximum	2.47	23.20
	Minimum	0.62	0.20
Autumn 2014	Average	1.02	0.67
	Maximum	1.55	11.99
	Minimum	0.72	0.00
Summer 2015	Average	1.04	1.10
	Maximum	2.47	12.39
	Minimum	0.62	0.00
Winter 2015	Average	1.03	6.17
	Maximum	2.06	23.20
	Minimum	0.64	0.20



Table 4. Concentration of TEP in 0-50m depths at different area from various reports.

Location	CTEP ($\mu\text{g Xeq. L}^{-1}$)	References
Santa Barbara Low Strait	85-252	Passow and Alldredge (1995)
The Baltic Sea	145-322	Engel (2002)
Gulf of Cadiz	25-717	Garc et al. (2002)
Eastern North Atlantic	20-60	Engel (2004)
Adriatic Sea	4-14800	Radic et al. (2005)
Western subarctic North Pacific	40-190	Ramaiah et al. (2005)
Arabian Sea	507-560	Prieto et al. (2006)
Jiulong river estuary	530-720	Peng and Huang (2007)
Weddell Sea	0-48.9	Ortega-Retuerta et al. (2009)
Newson Estuary	805-1801	Wetz et al. (2009)
Gulf of Aqaba	130-222	Bar-Zeev et al. (2009)
Pearl River Estuary	85-1235	Sun et al. (2010)
Mediterranean Sea	19.4-53.1	Ortega-Retuerta et al. (2010)
Eastern tropical North Pacific	22.5	Wurl et al. (2011b)
Eastern Mediterranean Sea	116-420	Bar-Zeev et al. (2011)
Eastern subarctic North Pacific	28.7	Wurl et al. (2011b)
Chesapeake Bay	37-2820	Malpezzi et al. (2013)
Western tropical North Pacific	43.3	Kodama et al. (2014)
Changjiang Estuary	173.33-1423.33	Guo & Sun (2018)
Bohai Sea	0.19-14.75	This Study (2014-15)
North Yellow Sea	0.19-23.20	This Study (2014-15)
South Yellow Sea	0.19-11.99	This Study (2014-15)



Table 5. Concentration of TEP in 50-100 depths at different area from various reports.

Location	CTEP ($\mu\text{gXeq. L}^{-1}$)	References
Gulf of Aqaba	106-228	Bar-Zeev et al. (2009)
Mediterranean Sea	9.1-94.3	Ortega-Retuerta et al. (2010)
Eastern tropical North Pacific	9.2	Wurl et al. (2011b)
Eastern Mediterranean Sea	48-189	Bar-Zeev et al. (2011)
Eastern subarctic North Pacific	11.6	Wurl et al. (2011b)
Western tropical North Pacific	42.2	Kodama et al. (2014)
Bohai Sea	0.39-4.33	This Study (2014-15)
North Yellow Sea	0.19-11.01	This Study (2014-15)
South Yellow Sea	0.2-0.79	This Study (2014-15)



Table 6. Average concentrations of TEP at different depths in different area.

Location	Water layer (m)	CTEP ($\mu\text{g Xeq. L}^{-1}$)	References
Santa Barbara Low Strait	0-75	29-68	Passow and Alldredge (1995)
Ross Sea	0-150	1003-7667	Hong et al. (1997)
Northwest Atlantic	10--70	10-120	Engle (2004)
Bransfield Strait	0-100	0-346	Corzo et al. (2005)
Gulf of Aqaba	100<	23-209	Bar-Zeev et al. (2009)
Mediterranean Sea	100<	4.5-23.5	Ortega-Retuerta et al. (2010)
Eastern Mediterranean Sea	100<	83-386	Bar-Zeev et al. (2011)
North Bering Sea	-	34-628	Lili et al. (2012)
Changjiang Estuary	0-100	321.52	Guo & Sun 2018
Bohai Sea	1-100	0.2-14.75	This Study (2014-15)
North Yellow Sea	1-100	0.2-23.20	This Study (2014-15)
South Yellow Sea	1-100	0.19-11.99	This Study (2014-15)



Table 7. Variations of Sinking rates of TEP and related applied methods from different reports.

Location	Sinking rate of TEP (m d^{-1})	Method	References
Santa Barbara Strait	-0.22-0.04	SETCOL	Azetsu-Scott 2004
South Pacific Ocean	-0.29~0.49	SETCOL	Mari 2008
Freshwater Lake Quéntar	1.12~1.31	Sediment Trap	Vicente 2009
Changjiang Estuary	0.08-1.08	SETCOL	Guo & Sun 2018
Bohai Sea	0.64~2.06	SETCOL	This Study (2014-15)
North Yellow Sea	0.72~2.47	SETCOL	This Study (2014-15)
South Yellow Sea	0.62~2.40	SETCOL	This Study (2014-15)



Table 8. Seasonal average TEP distribution in surface area from various research with their minimum to maximum ranges.

Seasons	Location	CTEP ($\mu\text{g Xeq. L}^{-1}$)			References
		Minimum	Maximum	Average	
Autumn	Bohai Sea	0.00	0.98	0.42	This Study (2014-15)
	North Yellow Sea	0.00	2.75	0.44	This Study (2014-15)
	South Yellow Sea	0.00	11.99	0.93	This Study (2014-15)
Spring	Changjiang Estuary	173.33	840.00	506.67	Guo & Sun 2018
	Northeast coast of Japan	901.00	1142.00	1021.50	Ramaiah et al. 2001
	Southern Iberian coasts	507.00	560.00	533.50	Prieto et al. 2006
Summer	Changjiang Estuary	473.33	1423.33	948.33	Guo & Sun 2018
	Baltic Sea	145.00	322.00	233.50	Engel 2002
	Northeast Atlantic Ocean	10.00	120.00	65.00	Engel 2004
	Bransfield Strait	0.00	346.00	173.00	Corzo et al. 2005
	Jiulong estuary	530.00	720.00	625.00	Peng and Huang 2007
	Pearl River estuary	85.00	1235.00	660.00	Sun et al. 2010
	Bohai Sea	0.00	12.39	1.02	This Study (2014-15)
	North Yellow Sea	0.00	6.49	0.83	This Study (2014-15)
	South Yellow Sea	0.00	10.22	1.42	This Study (2014-15)
Winter	Bohai Sea	0.20	14.75	4.82	This Study (2014-15)
	North Yellow Sea	0.39	23.20	7.00	This Study (2014-15)



Table 9. Seasonal average sedimentation rates of TEP in different locations with their maximum and minimum ranges from different reports.

Seasons	Location	TEP sinking rates (mD^{-1})			References
		Minimum	Maximum	Average	
Autumn	Bohai Sea	0.72	1.16	0.90	This Study (2014-15)
	North Yellow Sea	0.76	1.19	0.95	This Study (2014-15)
	South Yellow Sea	0.78	1.55	1.13	This Study (2014-15)
Spring	Changjiang Estuary	0.08	0.57	0.33	Guo & Sun 2018
Summer	Changjiang Estuary	0.10	1.08	0.59	Guo & Sun 2018
	Bohai Sea	0.86	1.57	1.01	This Study (2014-15)
	North Yellow Sea	0.77	2.47	1.06	This Study (2014-15)
	South Yellow Sea	0.62	2.4	1.05	This Study (2014-15)
Winter	Bohai Sea	0.64	2.06	1.02	This Study (2014-15)
	North Yellow Sea	0.72	1.53	1.03	This Study (2014-15)

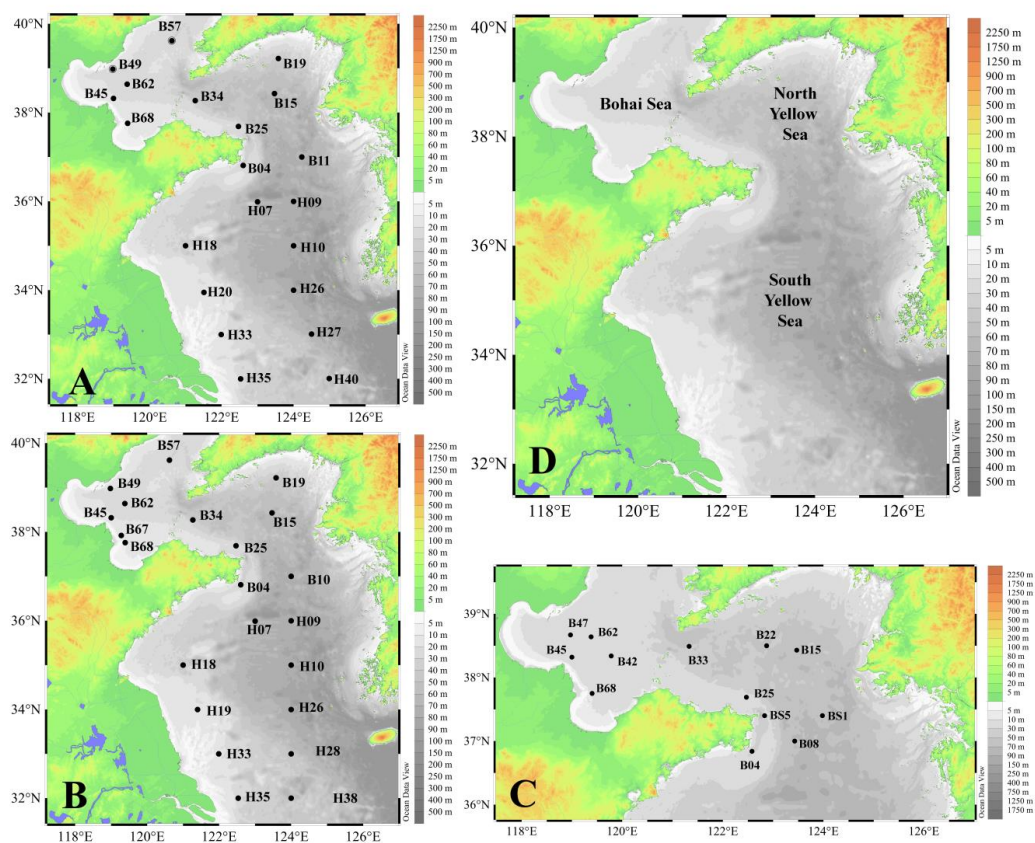


Figure 1. Study stations in map of autumn 2014 (A), summer 2015 (B) and winter 2015 (C) with their oceanic segmentation (D).

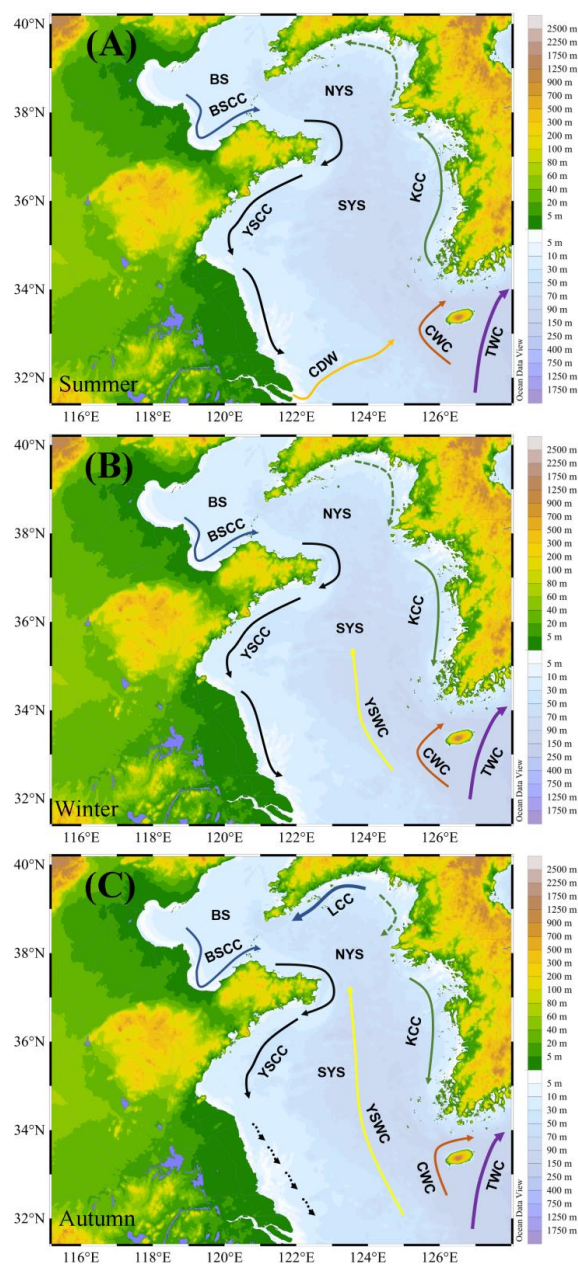


Figure 2. Direction of Currents at Bohai Sea (BS=Bohai Sea, BSCC=Bohai Sea coastal current), North Yellow Sea (NYS=North Yellow Sea, KCC=Korean Coastal Current, LCC=Liaonan coastal current, YSCC=Yellow Sea Coastal Current) and South Yellow Sea (SYS=South Yellow Sea, YSWC=Yellow Sea Warm Sea, CDW=Changiang Diluted Water,



CWC= Cheju Warm Current, TWC=Tsushima Warm Current) during summer (a), winter (b) and autumn (c) seasons (Collaboratively modified after Hwang et al. 2014; Su 1998; Yuan et al. 2008; Isobe 2008, Zhang et al. 2003).

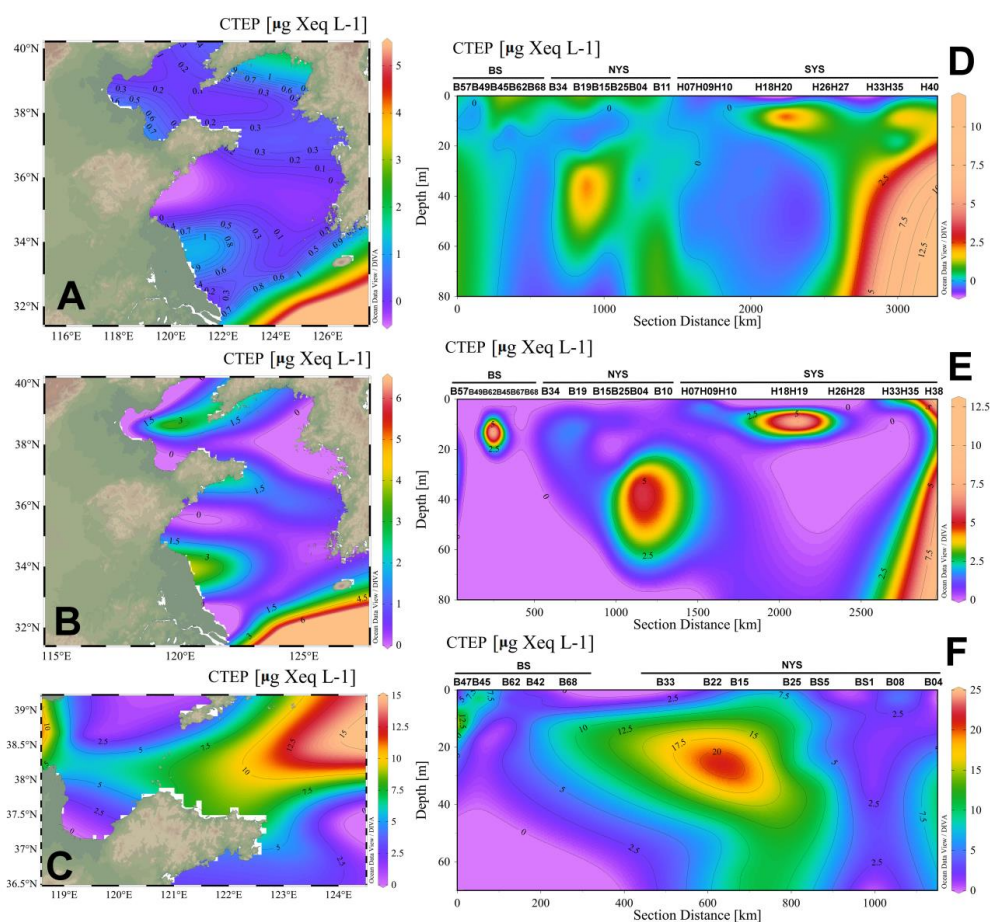


Figure 3. Average seasonal concentrations of CTEP (A, B & C) with sectional view (D, E & F) of BS (D), NYS (E) and SYS (F) during autumn (A), summer (B) and winter (C).

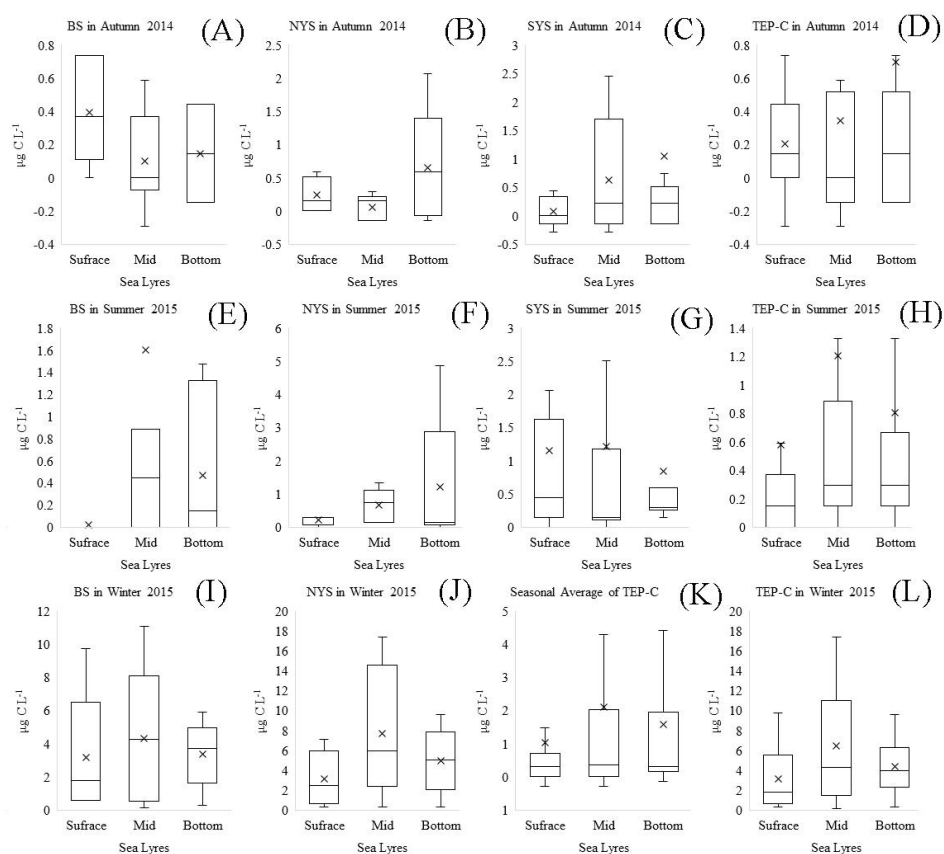


Figure 4. TEP associated carbon concentration during all seasons in Bohai Sea (A=autumn 2014, E=summer 2015, I=winter 2015), North Yellow Sea (B=autumn 2014, F=summer 2015, J=winter 2015), South Yellow Sea (C=Autumn 2014, G=summer 2015) with all data in average (K), autumn 2014 (D), summer 2015 (H) and winter 2015 (L).

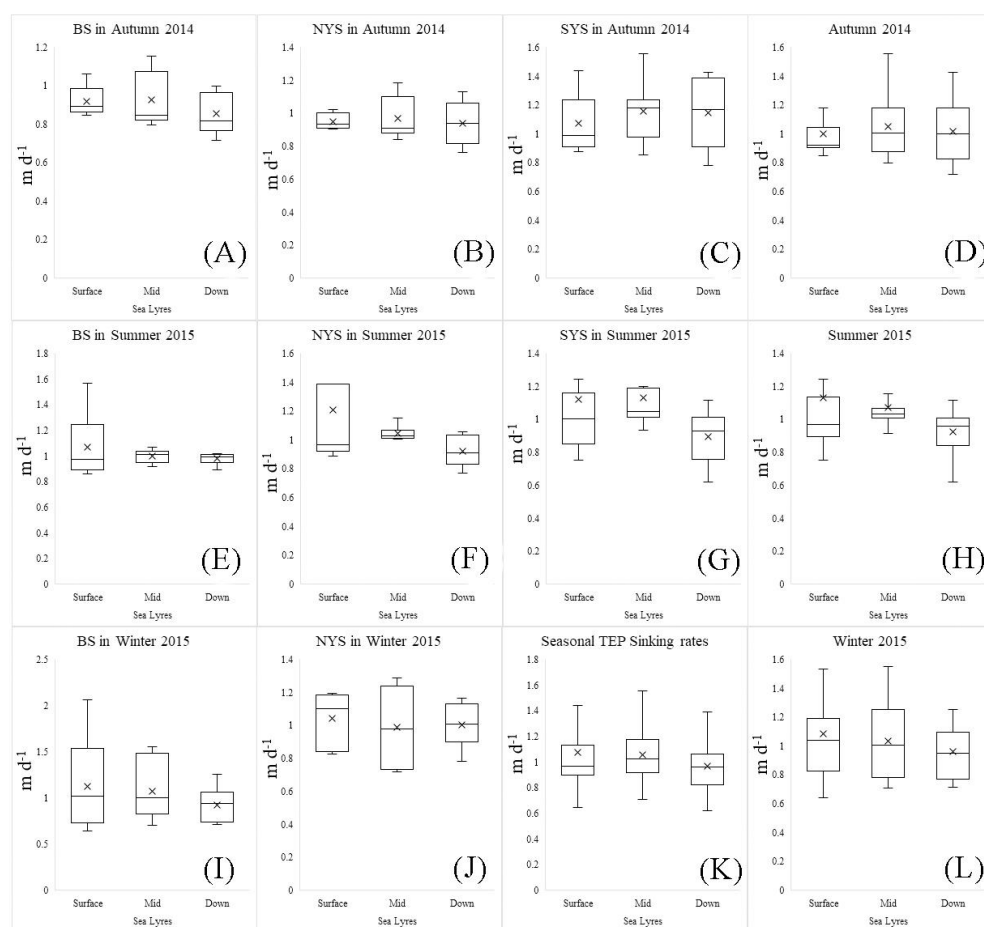


Figure 5.TEP sinking flux during all seasons in Bohai Sea (A=autumn 2014, E=summer 2015, I=winter 2015), North Yellow Sea (B=autumn 2014, F=summer 2015, J=winter 2015), South Yellow Sea (C=autumn 2014, G=summer 2015) with all seasonal sinking data in average (K), autumn 2014 (D), summer 2015 (H) and winter 2015(L).

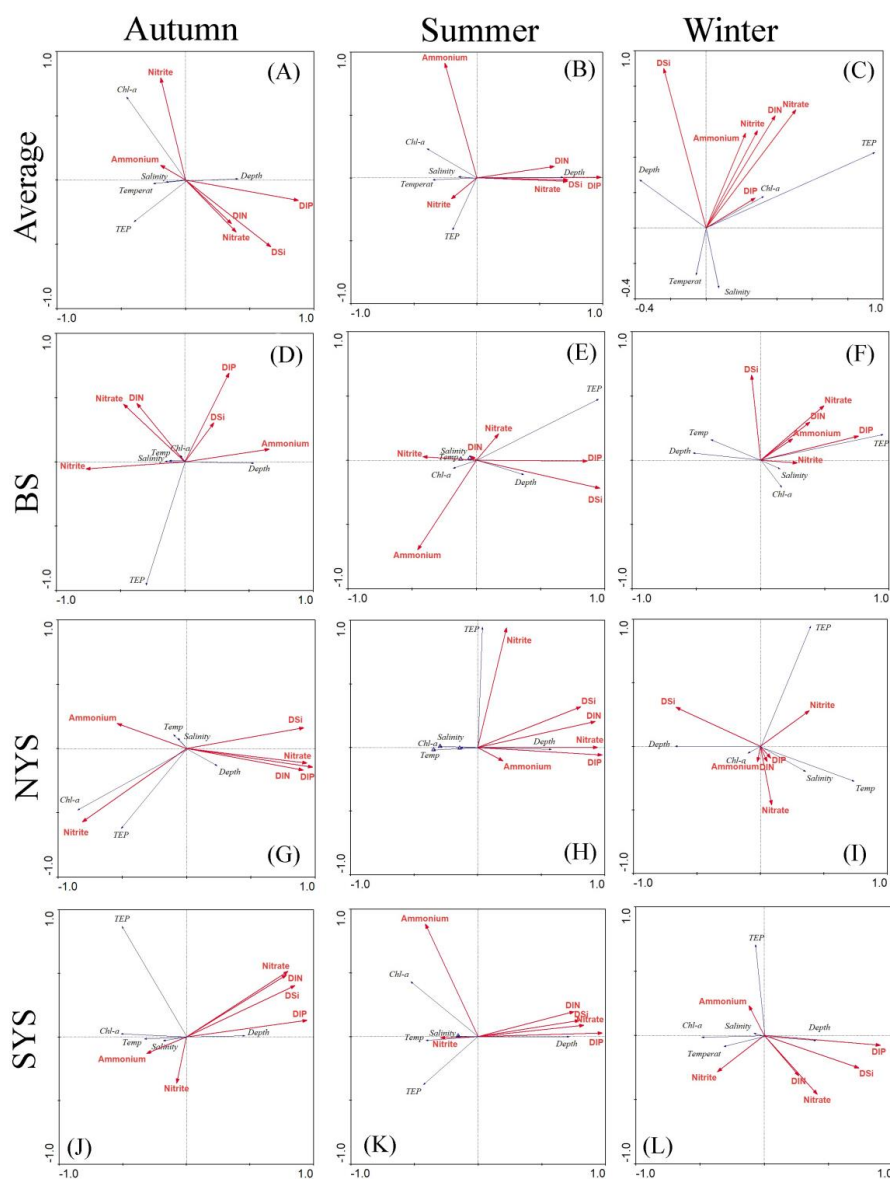


Figure 6. CCA analysis of all parameters of all study stations. Seasonal average i.e. autumn 2014 (A), summer 2015 (B), winter 2015 (C) and total (L) with the CCA of all parameters according to locations i.e. Bohai Sea (D=autumn 2014, E=summer 2015, F=winter 2015), North Yellow Sea (G=Autumn 2014, H=summer 2015, I=winter 2015) and South Yellow Sea (J=autumn 2014, K=summer 2015).

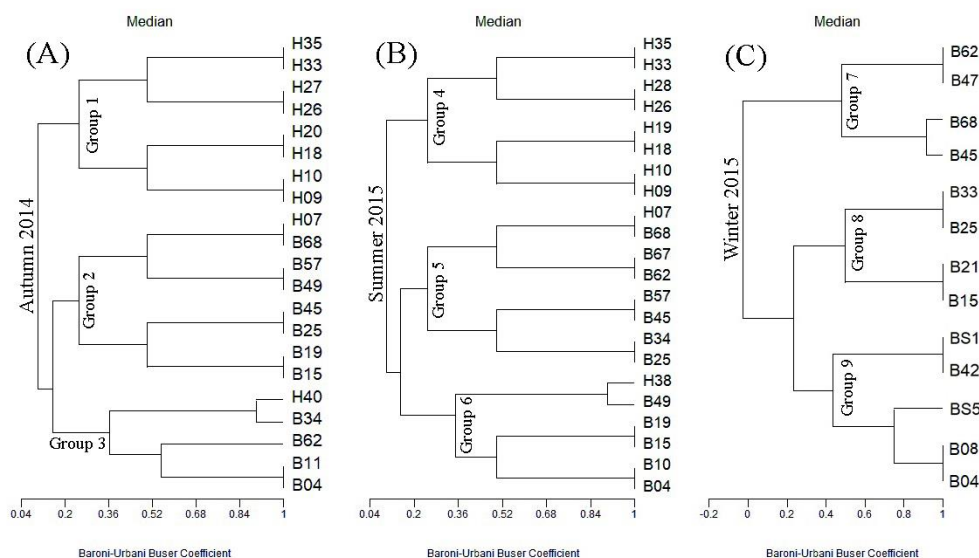


Figure 7. Seasonal Cluster analysis among related study stations of study area by considering all parameters and CTEP, segmented by seasons i.e. autumn 2014 (A), summer 2015 (B) and winter 2015 (C). Groups (1-9) are indicating clustered group of closely related stations.